

Effect of process parameters on the properties of ultrananocrystalline diamond films deposited using microwave plasma enhanced chemical vapor deposition

Vijay Chatterjee^{1,2*}, Rishi Sharma¹, P. K. Barhai¹

¹Department of Applied Physics, Birla Institute of Technology, Mesra, Ranchi 835215, India

²School of Chemistry, University of Bristol, Bristol BS8 ITS, United Kingdom

*Corresponding author. Tel: (+91) 9934113096; Fax: (+91) 6512275401; E-mail: vijay7chatterjee@gmail.com

Received: 06 October 2013, Revised: 10 November 2013 and Accepted: 17 November 2013

ABSTRACT

Ultrananocrystalline diamond (UNCD) films are deposited using microwave plasma enhanced chemical vapor deposition system. Depositions of films are carried out at low pressure 25 mbar, low temperature 400 °C and at low microwave power (800 - 1000 Watt). Diamond thin films were characterized using Raman spectroscopy, AFM, field emission scanning electron microscopy and optical contact angle measurements. In-situ diagnosis of the plasma composition is carried out using optical emission spectroscopy (OES). OES spectra show intense peak at 516.5nm corresponding to C₂ dimer. Peaks at 387.0nm, 405.3nm, 431.5nm, 486.1nm, and 656.1nm have also been observed. Effect of horizontal position of plasma ball with respect to substrate position has been critically analyzed. Relation between the horizontal positioning and plasma ball along with the emission spectra of different gas species are studied which are very much crucial to predict the uniformity and morphology of the films deposited. Dependence of film wettability with the plasma ball positioning and relative intensity of carbon dimer has been studied. C₂ dimer plays an important role not only in the nucleation and growth of UNCD films but also on the surface modification. Copyright © 2014 VBRI press.

Keywords: Ultrananocrystalline diamond; optical emission spectroscopy; C₂ dimer; plasma ball.



Vijay Chatterjee is presently pursuing his PhD in the department of Applied Physics, Birla Institute of Technology, Mesra, Ranchi. He received his M. Phil (Applied Physics) degree from Indian School of Mines, Dhanbad in 2009. His early research was based on studying optical properties of nanophosphors; his present research area is focussed to carbon and family. He worked in all area of carbon including diamond like carbon, nanocrystalline diamond, Ultrananocrystalline diamond, graphene etc. He is awarded the prestigious Commonwealth Scholarship in 2012 which makes him an integral part of, University of Bristol, School of Chemistry diamond group, United Kingdom.



Rishi Sharma is Assistant Professor in the Department of Applied Physics, Birla Institute of Technology, Mesra, Ranchi, India. He had completed M. Tech. in 2005 and Ph.D. in 2012. His present research interest is Ultrananocrystalline and Nanocrystalline Diamond thin films, Diamond-like Carbon films, Carbon nano tubes, Graphene and Dye sensitized solar cells. He has also visited University of Duisburg-Essen, Germany twice,

under DST-BMBF, Indo-German Bilateral Cooperation in Science & Technology to work on DLC and UNCD.



P. K. Barhai, Professor, Department of Applied Physics, Birla Institute of Technology, Mesra, Ranchi, India had done his M. Sc. in Physics in 1970 and Ph. D in Physical Sciences from Dibrugarh University in 1975. He joined BIT Mesra as an Assistant Professor in the Department of Applied Physics in 1976 and since then he has been serving in various capacities as Head of the Department, Dean Faculties & Sponsored Research and Vice-Chancellor. He has completed many R&D Projects supported by Indian Space Research Organization, Department of science and Technology, Government of India, Board of Research on Nuclear Science, Department of Atomic Energy, Govt. of India, All Indian Council for Technical Education, Aeronautical Research and Development Board, University Grants Commission, DST-BMBF (Indo-German) Project under Indo-German Bilateral Cooperation on Science and Technology, India-Israel Project under Indo-Israel Bilateral Cooperation on Science and Technology etc. He was a Visiting Scientist for two times under DST-BMBF at the University of Duisburg, Germany during 2008-10 and for three times at Tel Aviv University under Indo-Israel Project.

Introduction

Ultrananocrystalline diamond (UNCD) thin films have been finding many applications in recent years due to their excellent properties like phase purity, high hardness, chemical inertness, small crystal size and important mechanical properties such as high Young's modulus, fracture toughness and low coefficient of friction. They are also being considered for many electronic applications because of their wide band gap. Some of the important industrial applications are protective coatings, Micro-Electro-Mechanical-Systems (MEMS), surface acoustics wave devices (SAW) and as electron emitters in display devices.

Chemical vapor deposition technique is a well established method for the synthesis of thin film [1,2]. Electronic devices [3], protective coatings [4] and optical coatings [5] are routinely produced by CVD with excellent performance. Plasma CVD systems are different from other plasma assisted techniques such as rf induction [6-8], microwave (MPECVD) [9-12], filament (FECVD) [13-15], and dc plasma jet [16]. All of these methods have been used to synthesize diamond thin films. Each system has certain advantages with respect to diamond film deposition, for example MPECVD system produces films of high quality while dc plasma jet CVD has high growth rates [17-18]. There are varieties of diamond CVD techniques.

Hot filament reactor is widely used to deposit diamond thin films. The commonly used filament material is a kind of chemically-inert metal, e.g. tungsten or tantalum. However, under the high temperature, it will inevitably react with carbon-containing species and gradually degrade, and finally become more brittle and highly resistive. This then will influence both the power coupling efficiency and the catalysis activity. Also, due to the presence of the filament in the reactor, the input gas for HF-CVD cannot contain oxidizing or corrosive gases. Even so, the contamination from the filament material is still difficult to avoid. Thus, usually, HF-CVD-grown diamond has low quality and is suitable for mechanical, but not for electronic applications. Besides those drawbacks, the diamond growth rate by HFCVD is also low.

The DC arcjet is a commercial way to produce diamond. In the DC-arc jet, an anode and a cathode are connected by a DC power supply. Between the two electrodes a discharge region is formed. When gases such as an Ar/H₂/CH₄ mixture flow through this region, ionization occurs and a jet of plasma is generated and accelerated by a pressure drop towards the substrate, where the diamond film is deposited. The advantage of this technique is its high growth rate, however, this method cannot grow diamond over large areas and, again, metal contamination (from the cathode) tends to impair the diamond purity and quality.

Microwave (MW) plasma is now the most popular way to produce high quality diamond film. The two most common types of MWCVD reactor are shown in Fig. 1. In microwave plasma enhanced chemical vapor deposition (MPECVD) the feed gas mixture is ionized and excited by microwave power in a reaction chamber. Ionized and excited neutral atomic and molecular components form plasma, generally of low fractional ionization, in which

radicals and neutral reacts and/or recombine and condense onto the substrate as a thin film [19].

The advantage of this method is that there is no electrode or filament in the reactor. This provides a clean environment for diamond growth. Also, the diamond growth rate is relatively fast due to high input power and the immersion of the substrate into the plasma. Depending on the operational parameters such as gas composition, pressure and flow rate, substrate temperature and microwave power, thin film with the desired microstructure and mechanical properties can be produced reliably. The main drawback is that such systems are usually expensive. The system described here is a MPECVD facility used for the diamond thin – film deposition.

Here, we describe a simple, safe and economical microwave deposition system developed indigenously for producing high quality UNCD films. The microwave plasma facility has some additional features and improvements that could be advantageous to other similar systems. The microwave system is a 2.45 GHz, 3 kW (max with the matched load) systems driven by a magnetron that is operated at 50 Hz. Optimal deposition conditions are achieved when the plasma volume ignited in the low pressure chamber is hemispherical and located just above the substrate holder. An additional heating system is attached with the substrate holder, which allows us to control the substrate temperature. Two view ports are provided to measure the temperature of the substrate using an infrared pyrometer and the other to record the spectra using OES. The sample holder can be adjusted according to the plasma ball position which again depends on microwave power and pressure of the chamber. The main advantage of the system is this is complete manual yet wherever required safety interlocks are provided.

The optimal condition for the deposition of diamond thin growth has been critically analyzed. Correlation of plasma ball with the emission of feed gas in the chamber and relation of emission intensity of gas species with the film morphology has been studied.

Experimental

Material

Single side polished, single crystal, orientation <100> prime grade, resistivity in the range of 1-10 Ω-cm, silicon wafers for the experiments were purchased from PlasmaChem GmbH, Berlin. For the seeding of the sample PL-Nanopure- G, nanodiamond 4 wt% aqueous suspension, grade G were purchased from PlasmaChem GmbH, Berlin.

Methods

The schematic diagram of the microwave system is shown in Fig. 1. Microwave power enters the stainless steel reaction chamber from the top through a quartz window. The gas enters the chamber through a gas shower arrangement. The double walled chamber allows the system to remain sufficiently cool. The substrate can be viewed through a view port provided at the top. The substrate temperature can be measured by means of an infrared pyrometer. The substrate temperature is also measured by using a thermocouple.

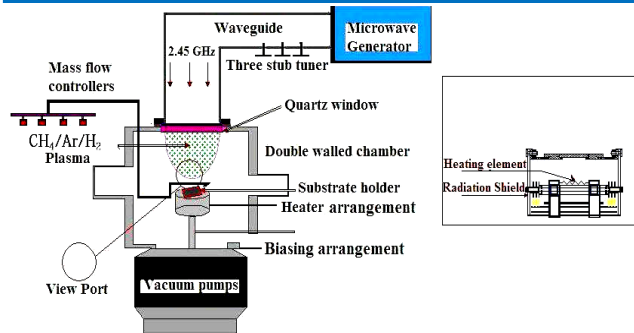


Fig. 1. The schematic diagram of the microwave PECVD unit.

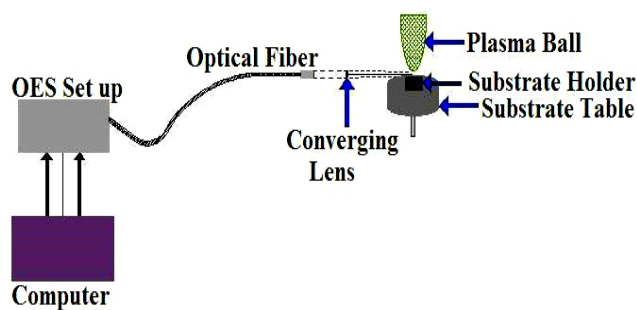


Fig. 2. The schematic diagram of the OES setup.

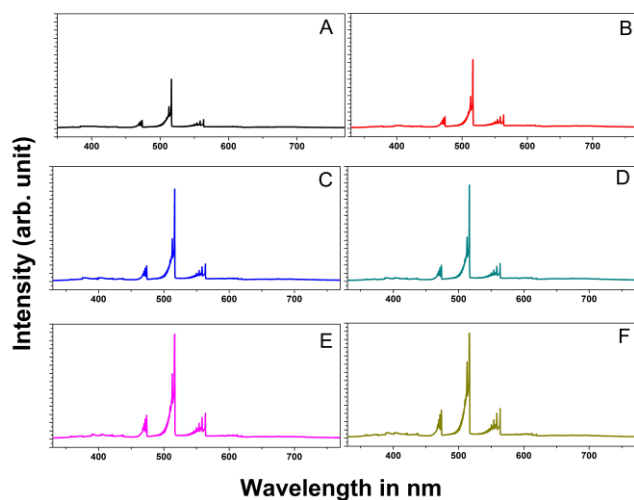


Fig. 3. OES Spectra of the plasma. position (A) at a distance 5 cm from the plasma ball at 800 W microwave power, (B) at a distance 5 cm from the plasma ball at 1000 W microwave power (C) at a distance 2.5 cm from the plasma ball at 800 W microwave power (D) at a distance 2.5 cm from the plasma ball at 1000 W microwave power (E) Directly under the plasma ball at 800 W microwave power (F) Directly under the plasma ball at 1000 W microwave power.

The microwave power dissipated in the stainless steel chamber is assumed to be small compared to that dissipated in the plasma. The three stub tuner was adjusted to minimize the microwave power reflectance which is typically less than 1% under methane plasma but can go up to 5% in hydrogen rich plasma. The system is equipped with safety interlocks. The substrate heater has a temperature controller which regulates the temperature required for deposition. The facility can run continuously without supervision after an initial stabilization period of ~15 min. After this period the substrate temperature, gas pressure, and microwave power level remain steady

throughout the experiment. The plasma characteristics of the microwave plasma enhanced CVD facility shows stability over a wide range of parameters. As soon as the system is stabilized, plasma is obtained in the form of a hemispherical ball in between the inlet of microwave at the top and the substrate holder. The lower edge of the plasma ball just touches the substrate. This adjustment of the plasma ball is very important for the deposition of good quality diamond films. The position of the plasma ball depends on the substrate position, the gas pressure and the microwave power.

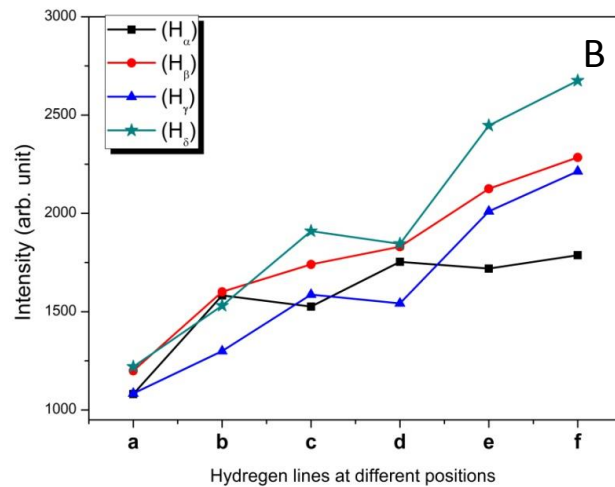
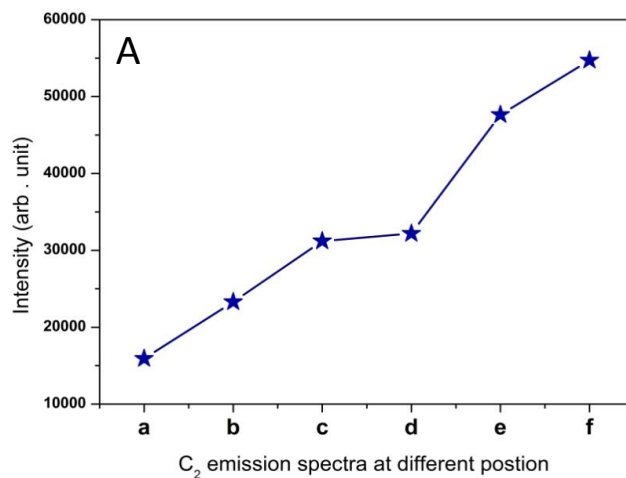


Fig. 4. (A) OES Spectra of the variation of intensity of C_2 with microwave power, (B) OES Spectra of the variation of intensity of H_δ , H_γ , H_β and H_α with microwave power.

Results and discussion

Prior to deposition the films were pretreated using Nanopure grade G, 4%, nanodiamond aqueous suspension. In this process we take 5 mg nanodiamond aqueous suspension with methyl alcohol and ultrasonicate it for one and half hour to make a uniform scratching of the surface of the substrate using diamond aqueous solution. The entire sample deposited undergoes the same method of pretreatment. The samples were then thoroughly ultrasonicated in methyl alcohol to assure no diamond residue is left sticking to the sample. For comparative purpose films were prepared with pretreatment and without pretreatment but, the results shows that even if some nuclei

grows on sample without pretreatment with diamond suspension the uniformity and density is very less compared to films deposited with pretreatment, so in order to grow sample with uniformity and good nuclei density it is required to pretreat the sample, there are other methods of pretreatment also like mechanical scratching, low pressure treatment, but in our case we use ultrasonication in diamond solution of the substrate, the reason for choosing this method is in mechanical scratching of the sample the substrate damage may occur is not suitable for deposition of very thin film. While low pressure pretreatment has disadvantage of developing surface stress.

Optical emission spectroscopy

The schematic diagram of the Optical emission spectroscopy set up has been shown in **Fig. 2**. The optical emission spectra were recorded at different position with respect to the plasma position during deposition of diamond films as shown in **Fig. 3** (A-F). All the recorded OES spectra shows vibrational transition at 516.3 nm corresponding to intense green color discharge attributed to the emission of the C₂ dimer corresponding to the swan system (0, 0), two other bands at 473.7 and 563.5 are because of C₂ (0, 1) and C₂ (1, 0) systems, respectively [20]. Peaks at 387.0nm, 405.3nm, 431.5nm, 486.1nm, and 656.1nm have also been observed. C₂ emission intensity is directly proportional to the concentration of C₂ dimer in the plasma. Higher the intensity, higher is the concentration of C₂ radical in the plasma. The variation of intensities of C₂, H_α, H_β, H_γ and H_δ with respect to different position with the plasma ball has been shown in **Fig. 4** (A-B).

The plots reveal that C₂, H_α, H_β, H_γ and H_δ emission changes with change in plasma ball position. Intensity of the emission spectra decreases on either side of the horizontal position with respect to the plasma ball. At a position 5 cm away from the plasma ball the generation of C₂ is low; rate of decomposition is also low and over all intensity of C₂ and other gas species are low, while at a distance 2.5 cm the rate of generation of C₂ and other species are higher compared to 5cm so the intensity of species are higher with respect to 5 cm away from the plasma ball position. At a position directly under the plasma ball the rate of generation of all the species are much higher of all species compared to different positions. At a position directly under the plasma ball the rate of the generation of C₂ and other species is more than their decomposition compared to other positions. So, we conclude on either side of the plasma ball the intensity of the gas species decreases and this directly affects the films quality.

Table 1. Transition level of different spectral lines.

Sl. No.	Species	Transition	peak position (nm)
1.	H _δ	n'=6→n=2	410.2
2.	H _γ	n'=5→n=2	434.0
3.	H _β	n'=4→n=2	486.1
4.	H _α	n'=3→n=2	656.1
5.	C ₂	d ³ Πg→a ³ Πu	516.3

The kinetics of C₂ formation strongly depends on gas temperature as in the position directly under plasma ball

increases the temperature of the gas this increases and formation of C₂ and other species. This shows that the generation and decomposition of the species strongly depends on plasma ball position. The transition levels of the species have been shown in **Table 1**.

Relation between microwave power and plasma density

The plasma density n_e may be obtained from the dissipation of input power into the plasma by using the expression as given by Weng et al. [21]

$$kP = e^2 n_e E^2 / (m_e v_m), \quad (1)$$

Where P is the microwave power, k is the microwave power absorption coefficient in the plasma, E is the effective electric field and v_m is the momentum transfer collision frequency. As seen from **Eq. (1)**, the plasma density increases with increase in the incident microwave power. Uhm et al. [22] have shown that at constant electron density and electron temperature, the ion energy increases with the microwave power;

$$n_e \sqrt{T_e \epsilon_L} \sim kP \quad (2)$$

Where T_e represents electron temperature in eV and ε_L indicates the energy dissipated in the plasma per ion injected in the plasma sheath. ε_L can be written as;

$$\epsilon_L = \epsilon_c + 2T_e + \epsilon_i \quad (3)$$

Where ε_c is the energy lost by collision and ε_i is the ion energy gained in the plasma sheath.

OES spectra recorded during the deposition shows that with increase in microwave power the intensity of the emission of the corresponding gas species increases. At higher power the pressure of the chamber also increases. We find that as the power increases the chamber pressure, the electron temperature, the plasma potential and the ion energy decreases and at the same time it increases the plasma density and radical concentration which is an essential condition for the deposition of film with enhanced growth rate.

The position of the substrate corresponding to the plasma ball has been found to be very crucial as even if all the conditions are satisfied, there will be variation in the film morphology with change in the position with respect to the plasma ball. The comparative changes in the morphology of the sample are shown in (**Fig. 9**). Three different conditions have been explored and the corresponding results show vital information on the importance of the position of plasma ball. Detail analysis of the plasma ball position with C₂ emission intensity shows that even with the same position of the plasma ball, the one with high intensity of C₂ produces more uniform film.

Raman spectra

Raman spectra of UNCD films deposited on silicon substrate at different experimental conditions are shown in **Fig. 5**. The results agree well with previously reported spectra [23 - 25]. Three prominent peaks are observed at

1140, 1335 and 1580 cm^{-1} . The broad peaks at 1335 and 1580 cm^{-1} are commonly termed as D band and G band, respectively. The peak at 1140 cm^{-1} is assigned to nano-crystalline diamond films [26, 27].

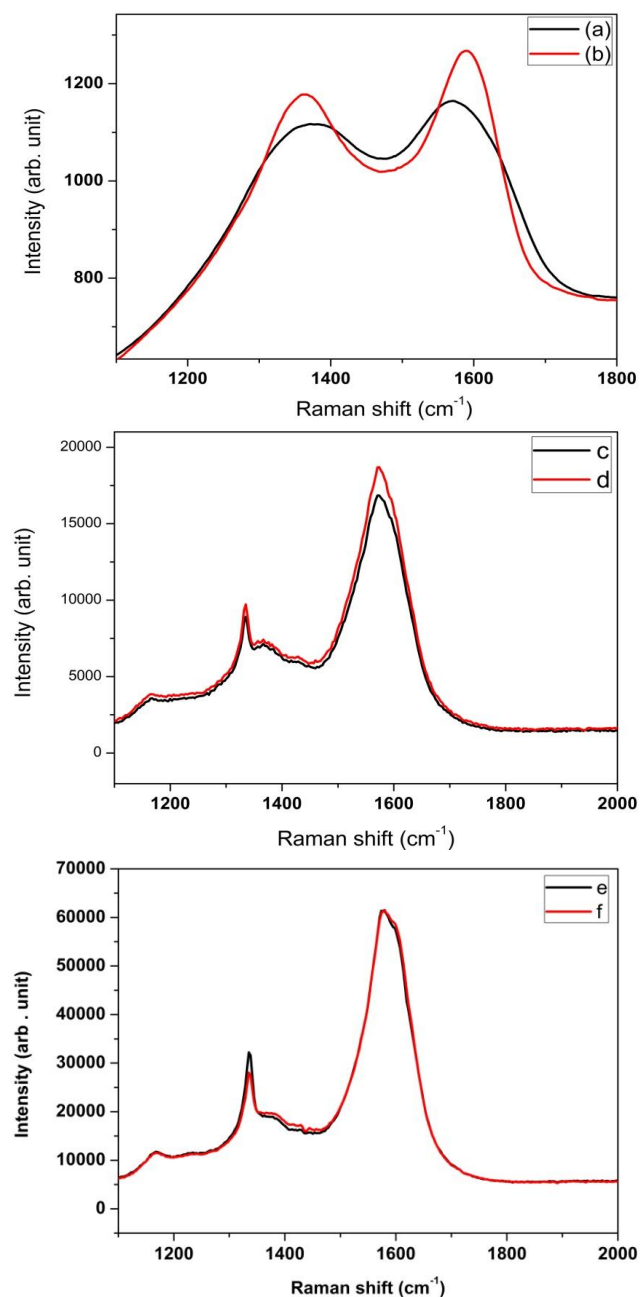


Fig. 5. Raman spectra of the UNCD films at different position with respect to plasma position (A) at a distance 5 cm from the plasma ball at 800 W microwave power, (B) at a distance 5 cm from the plasma ball at 1000 W microwave power (C) at a distance 2.5 cm from the plasma ball at 800 W microwave power (D) at a distance 2.5 cm from the plasma ball at 1000 W microwave power (E) Directly under the plasma ball at 800 W microwave power (F) Directly under the plasma ball at 1000 W microwave power.

However, there is certain ambiguity in this peak. Ferrari and Robertson [28] and Kuzmany et. al. [29] assigned the peak at 1140 cm^{-1} to transpolyacetylene segments present at the grain boundaries and surfaces of nano-diamond films. However, this peak is generally observed in both UNCD and NCD films [24, 25]. Since the sp^2 -bonded carbon is

highly sensitive to visible Raman spectroscopy than sp^3 -bonded carbon, sharp peak at 1332 cm^{-1} was not observed. The formation of transpolyacetylene also suppresses the intensity of this peak.

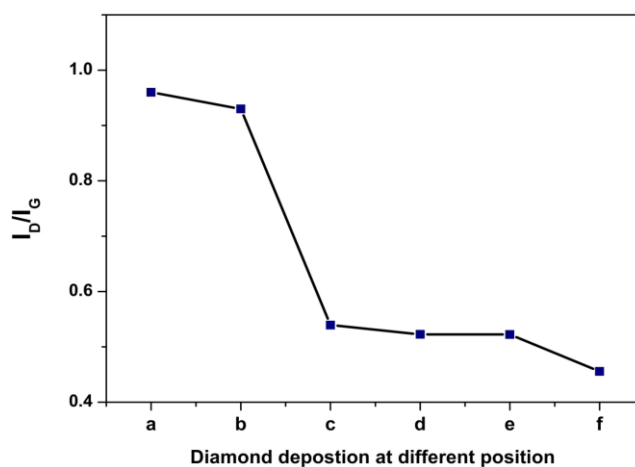


Fig. 6. I_d/I_g ratios of the sample at different positions (a) at a distance 5 cm from the plasma ball at 800 W microwave power, (b) at a distance 5 cm from the plasma ball at 1000 W microwave power (c) at a distance 2.5 cm from the plasma ball at 800 W microwave power (d) at a distance 2.5 cm from the plasma ball at 1000 W microwave power (e) Directly under the plasma ball at 800 W microwave power (f) Directly under the plasma ball at 1000 W microwave power.

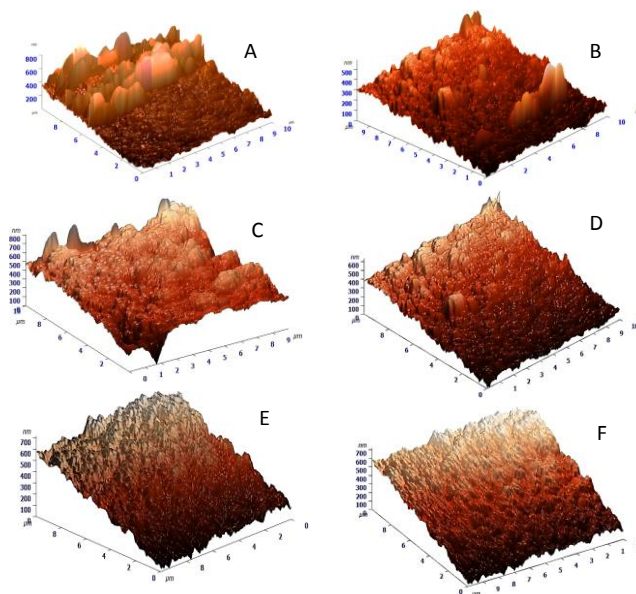


Fig. 7. Atomic force image of films at different position with respect to plasma. (A) At a distance 5 cm from the plasma ball at 800 W microwave power, (B) At a distance 5 cm from the plasma ball at 1000 W microwave power (C) At a distance 2.5 cm from the plasma ball at 800 W microwave power (D) At a distance 2.5 cm from the plasma ball at 1000 W microwave power (E) Directly under the plasma ball at 800 W microwave power (F) Directly under the plasma ball at 1000 W microwave power.

Fig. 6 shows the I_d/I_g ratio of diamond thin films deposited at different position with respect to the plasma ball. It is shown in the fig that the I_d/I_g ratio decreases as we change the position ultimately the carbon dimer intensity here we conclude that one deposited just under the Plasma ball at 1000 W has the lower ration compared to the one at 800 W at 5cm from the plasma. I_d/I_g ratio is a

measure of the grain size lower the ratio lower is the crystallite size.

Atomic force microscopy

The atomic force microscopy (AFM) images of the sample were taken and shown in **Fig. 7** from the AFM image it is evident that the morphology of the sample varies greatly with respect to the position of the plasma ball. The films deposited at 5 cm away from the plasma ball are non uniform and also the grains are not small as compared to one deposited at 2.5 cm or directly under the plasma ball. The one prepared at 2.5 cm away from the plasma ball are relatively uniform compared to deposited at 5 cm away from plasma ball but they are non uniform compared to the one deposited under the plasma ball. The one deposited directly under the plasma ball are uniform compared to both the positions also the contact angle measurement provides further evidence to this result. The grain size, uniformity and roughness of the samples depend on the plasma ball position.

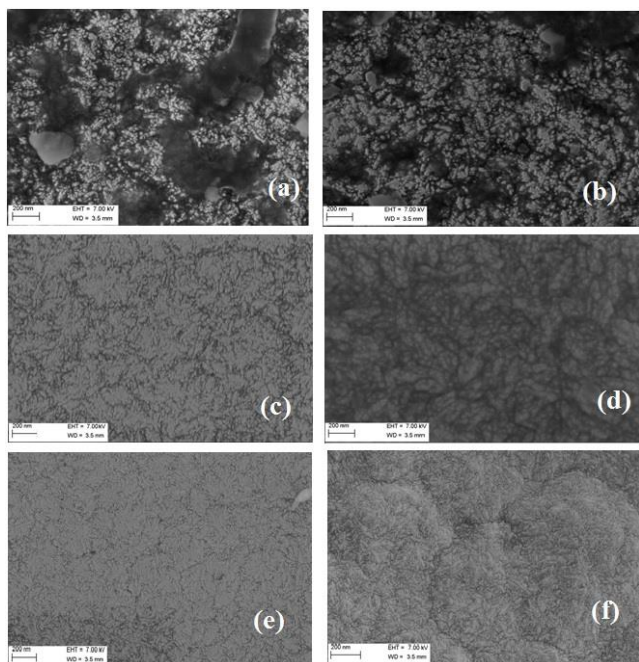


Fig. 8. SEM images of samples at different position with respect to plasma. (a) At a distance 5 cm from the plasma ball at 800 W microwave power, (b) At a distance 5 cm from the plasma ball at 1000 W microwave power (c) At a distance 2.5 cm from the plasma ball at 800 W microwave power (d) At a distance 2.5 cm from the plasma ball at 1000 W microwave power (e) Directly under the plasma ball at 800 W microwave power (f) Directly under the plasma ball at 1000 W microwave power.

Field emission scanning electron microscopy (FESEM) analyses

The FESEM results of the samples are shown in **Fig. 8 (a-f)**. The results show the effect of the position of sample with respect to the plasma ball. The detail morphological study of the films deposited at different horizontal position with respect to the plasma ball has been studied. The samples were placed at three different positions from the plasma ball, they are respectively 5cm, 2.5 cm and the third one placed directly under the plasma ball. The experiments

were repeated for different microwave power. At higher power no deposition takes and few times samples get burnt and at lower power very poor nuclei growth takes place. We present a comparison of films deposited at 800 W and 1000 W keeping all other parameters including distance from plasma ball constant. The film morphology shows that plasma ball position is very important for the film deposition as the FESEM image for samples at 5cm away for 800 W and 1000 W deposited samples shows non uniformity of the samples also the roughness of the samples are very high compared to other positions close to the plasma ball.

The films deposited at a position 2.5 cm away from the plasma are uniform compared to films deposited at 5 cm but they are non uniform and rough compared to the films deposited at a position directly under the plasma ball. The SEM reveals that substrate position with respect to plasma ball plays a very crucial role in film deposition. The SEM results also confirm very good rate of deposition for samples placed under directly under the plasma ball. Here we can also conclude that the intensity of C_2 is higher just at the bottom of the plasma ball compared to other distances which results in higher nucleation rate. FESEM reveals that the uniformity of the film strongly depends on the microwave power, gas composition ratio, position of the plasma and the time of deposition.

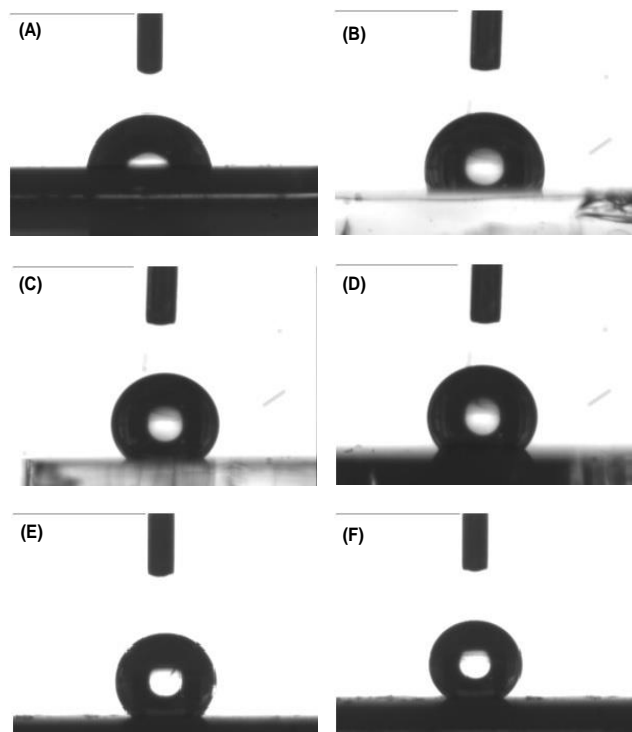


Fig. 9. Optical contact image of samples deposited (A) At a distance 5 cm from the plasma ball at 800 W microwave power, (B) At a distance 5 cm from the plasma ball at 1000 W microwave power, (C) At a distance 2.5 cm from the plasma ball at 800 W microwave power, (D) At a distance 2.5 cm from the plasma ball at 1000 W microwave power, (E) Directly under the plasma ball at 800 W microwave power and (F) Directly under the plasma ball at 1000 W microwave power.

Optical contact angle measurement

The contact angle is measured by a contact angle setup (Data physics, Germany). The optical contact angle (OCA)

of the samples with water is studied. All the measurements were performed at room temperature and humidity was maintained constant. The contact angle measurements were repeated to check reproducibility. The result reveals that the contact angle for UNCD coated Silicon with water lies between 98° and 141° which is higher compared to uncoated silicon (65°). The contact angle measurement of the sample shows significant change with variation in deposition position with respect to the plasma ball. It is observed that sample deposited at microwave power of 1000W under the plasma ball shows contact angle of 141° which proves that the film surface is hydrophobic. The variation of contact angle with different position with respect to plasma ball is shown in **Fig. 9 (a-f)**. The surface free energy of the all the sample has been calculated using equation of state formula (EOS).

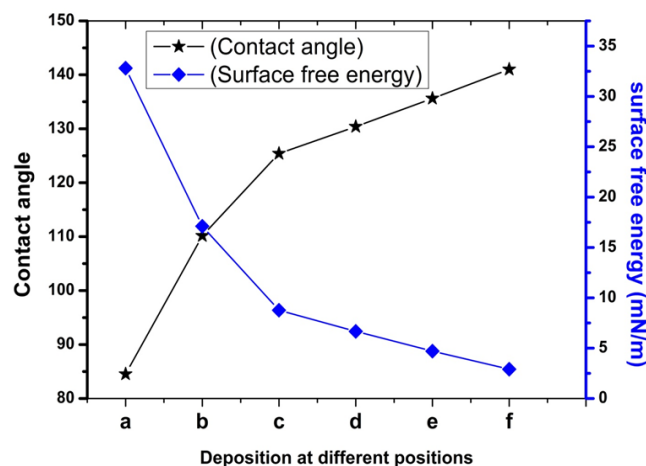


Fig. 10 Plot of variation of contact angle and surface free energy (a) at a distance 5 cm from the plasma ball at 800 W microwave power, (b) At a distance 5 cm from the plasma ball at 1000 W microwave power (c) At a distance 2.5 cm from the plasma ball at 800 W microwave power (d) At a distance 2.5 cm from the plasma ball at 1000 W microwave power (e) Directly under the plasma ball at 800 W microwave power (f) Directly under the plasma ball at 1000 W microwave power.

Table 2. Variation of contact angle and surface free energy with deposition power.

Sl. No	Deposition at different position	Contact Angle	Surface free energy SFE (mN/m)
1.	Pure silicon (Substrate) not shown	65.4	44.54
2.	a	84.53	32.8
3.	b	110.16	17.1
4.	c	125.4	8.77
5.	d	130.4	6.67
6.	e	135.63	4.71
7.	f	141	2.91

(a = 5 cm away from plasma ball at 800 W, b = 5 cm away from plasma ball at 1000 W, c = 2.5 cm away from plasma ball at 800 W, d = 2.5 cm away from plasma ball at 1000 W, e = directly under plasma ball at 800 W, f = directly under plasma ball at 1000 W).

In **Fig. 10** it is shown that surface free energy of the sample deposited at 1000 W directly under the plasma ball

has got the minimum value. The results shows that contact angle of the films depend on the deposition power and plasma ball position. It can be concluded that high intensity of C_2 affects the film response to wettability. **Table 2** shows the variation of contact angle and surface free energy with microwave power used for deposition.

Conclusion

The microwave plasma enhanced CVD facility described here allows depositing good quality diamond films with very low microwave power. The position of plasma ball corresponding to the position of substrate holder plays a key role in producing uniform coating of the films. The microwave power greatly influences the intensity of the emission lines of the gas species which is important for the development of good quality diamond films. The role of C_2 is very crucial as it has been shown that with the same position of the plasma ball with respect to the substrate, intense C_2 produces more uniform film compared to less intense C_2 . It is proved that intense C_2 can affect the wettability of the UNCD films.

Acknowledgements

This work was sponsored by the Department of Science and Technology (DST) New Delhi under Science and Engineering Research Council Grant no SR/S2/HEP-20/2008. We are grateful to Dr. S. Pradhan of IMMT, Bhubaneswar for the Raman and the FESEM data.

Reference

- Huang, W. S; Tran, D. T; Asmussen, J; Grotjohn, T. A; Reinhard, D. *Diamond & Related Material*, (2006); 15: 341.
DOI: [10.1016/j.diamond.2005.09.027](https://doi.org/10.1016/j.diamond.2005.09.027)
- Rovere, M; Porro, S; Musso, S; Shames, A; Williams, O; Bruno P; Tagliaferro, A; Gruen, D. M. *Diamond and Related Materials* (2006); 15:1913.
DOI: [10.1016/j.diamond.2006.07.013](https://doi.org/10.1016/j.diamond.2006.07.013)
- Jiao, S; Sumant, A; Kirk, M. A; Gruen, D. M; Krauss, A. R; and Auciello, O. *J. Appl. Phys.*, (2001); Vol 90, Num 1:118.
DOI: [10.1063/1.1377301](https://doi.org/10.1063/1.1377301)
- Shamsa, M; Ghosh, S; Calizo, I; Ralchenko, V; Popovich, A; and Balandin, A. A. *J. Appl. Phys* (2008);103:083538.
DOI: [10.1063/1.2907865](https://doi.org/10.1063/1.2907865)
- Ong, T. P; and Chang, R. P. H. *Appl. Phys. Lett.* 55, 2063 (1989); 2063.
DOI: [10.1063/1.102106](https://doi.org/10.1063/1.102106)
- Matsumoto, S. *J. Mater. Sci.* 4, 600 (1985).
DOI: [10.1007%2FBF00720043](https://doi.org/10.1007%2FBF00720043)
- Matsumoto, S; Hino, M; and Kobayashi, T. *Appl. Phys. Lett.* (1987); 51:737.
DOI: [10.1063/1.98851](https://doi.org/10.1063/1.98851)
- Sugai, H; Kojima, H; Ishida, A; and Toyoda, H. *Appl. Phys. Lett.* (1990); 56:2616.
DOI: [10.1063/1.103264](https://doi.org/10.1063/1.103264)
- Kuzmany, H; Pfeiffer, R; Salk, N; Gunther, B. *Carbon* (2004); 42:911.
DOI: [10.1016/j.carbon.2003.12.045](https://doi.org/10.1016/j.carbon.2003.12.045)
- Prins, Johan F. *Physical review B*, (2000); 61, Num 11.
DOI: [10.1103/PhysRevB.61.7191](https://doi.org/10.1103/PhysRevB.61.7191)
- May, P.W; Harvey, J.N; Smith, J.A; and Mankelevich, Yu. A. *J. Appl. Phys.*, (2006); 99: 104907.
DOI: [10.1063/1.2195347](https://doi.org/10.1063/1.2195347)
- Okano, K; Koizumi, S; Silva, S. R; and Amaratinga, G. A. *J. Nature (London)*, (1996); 140.
DOI: [10.1038/381140a0](https://doi.org/10.1038/381140a0)
- Ku, Chen-Hao; Wu, Jih-Jen. *Carbon*, (2004); 42:2201.
DOI: [10.1016/j.carbon.2004.04.032](https://doi.org/10.1016/j.carbon.2004.04.032)
- Bhattacharyya, S; Auciello, O; Birrell, J; Carlisle, J. A; Curtiss, L. A; Goyette, A. N; Gruen, D. M; Krauss, A. R; Schlueter, J; Sumant, A; and Zapol, P. *Appl. Phys. Lett.*, (2001); 79, Num 10:1441.
DOI: [10.1063/1.1400761](https://doi.org/10.1063/1.1400761)

15. Gracio, J. J.; Fan, Q. H; and Madalen, J. C. *J. Phys. D: Appl. Phys.* (2010); 43:374017.
DOI: [10.1088/0022-3727/43/37/374017](https://doi.org/10.1088/0022-3727/43/37/374017)
16. Kurihara, K; Sasaki, K; Kawarda, M; and Koshino, N. *Appl. Phys. Lett.* (1988); 52:437.
DOI: [10.1063/1.99435](https://doi.org/10.1063/1.99435)
17. Chen, G. C; Li , B; Li , H; Lan , H; Dai , F. W; Xue, Q. J; Han, X. Q; Hei, L. F; Song, J. H; Li, C. M; Tang, W. Z; and Lu, F. X. *Diamond & Related Material*, 19 (2010) 1078.
DOI: [10.1016/j.diamond.2010.03.012](https://doi.org/10.1016/j.diamond.2010.03.012)
18. Stalder, K. R; and Sharpless, R.L. *J. Appl. Phys.* (1990); 68:6187.
DOI: [10.1063/1.346909](https://doi.org/10.1063/1.346909)
19. Brewer, M. A; Brown, I. G; Dickinson, M. R; Galvin, J. E; MacGill, R. A; and Salvadori, M. C. *Rev. Sci. Instrum.* (1992), 63:3389.
DOI: [10.1063/1.1142557](https://doi.org/10.1063/1.1142557)
20. Gruen, D.M. 1999. Nanocrystalline diamond films. *Annu. Rev. Mater. Sci.* 29, 211.
DOI: [10.1146/annurev.matsci.29.1.211](https://doi.org/10.1146/annurev.matsci.29.1.211)
21. Weng, Y; Kushner, M. J. *Appl. Phys.* (1992); 72:33.
DOI: [10.1063/1.352144](https://doi.org/10.1063/1.352144)
22. Uhm, H. S; Lee, P. H; Kim, Y. I; Kim, J. H; Chang, H. Y. *IEEE Transaction on plasma physics* (1995); 23:628.
DOI: [10.1109/27.467984](https://doi.org/10.1109/27.467984)
23. Kulisch, W; Popov, C; Rauscher, H; Rinke, M; Veres, M; *Diamond & Related Materials*, (2011); 20:1076.
DOI: [10.1016/j.diamond.2011.03.042](https://doi.org/10.1016/j.diamond.2011.03.042)
24. Veres, M; Toth, S; Koos, M. *Appl. Phys. Lett.* (2007); 91,031913.
DOI: [10.1063/1.2757122](https://doi.org/10.1063/1.2757122)
25. Popov, C; Kulisch, W; Gibson, P.N; Ceccone, G; Jelink, M. *Diamond and Related. Mater.* (2004); 13:1371
DOI: [10.1016/j.diamond.2003.11.040](https://doi.org/10.1016/j.diamond.2003.11.040)
26. Joseph, P. T; Tai, Nyan-Hwa; Chen, Yi-Chun; Cheng, Hsiu-Fung; Lin, I-Nan. *Diamond & Related Materials* (2008); 17:476–480
DOI: [10.1016/j.diamond.2007.10.013](https://doi.org/10.1016/j.diamond.2007.10.013)
27. May, P. W; Ludlow, W. J; Hannaway, M; Heard, P. J; Smith, J. A; Rosser, K. N. *Diamond & Related Materials*, (2008); 17:105–117
DOI: [10.1016/j.diamond.2007.11.005](https://doi.org/10.1016/j.diamond.2007.11.005)
28. Ferrari, A. C; Robertson, J. *Phys. Rev. B* (2001); 075414.
DOI: [10.1103/PhysRevB.64.075414](https://doi.org/10.1103/PhysRevB.64.075414)
29. Kuzmany, H; Pfeiffer, R; Salk, B; Günther, B. *Carbon* (2004); 42:911
DOI: [10.1016/j.carbon.2003.12.045](https://doi.org/10.1016/j.carbon.2003.12.045)

Advanced Materials Letters

Publish your article in this journal

ADVANCED MATERIALS Letters is an international journal published quarterly. The journal is intended to provide top-quality peer-reviewed research papers in the fascinating field of materials science particularly in the area of structure, synthesis and processing, characterization, advanced-state properties, and applications of materials. All articles are indexed on various databases including [DOAJ](https://www.crossref.org/) and are available for download for free. The manuscript management system is completely electronic and has fast and fair peer-review process. The journal includes review articles, research articles, notes, letter to editor and short communications.

